



# Valorisation of vegetable oils via metathesis reactions on solid catalysts: Cross-metathesis of methyl oleate with 1-hexene



J. Zelin, P.D. Nieres, A.F. Trasarti, C.R. Apesteguía\*

Catalysis Science and Engineering Research Group (GICIC), INCAPE, UNL-CONICET, Predio CCT Conicet, Paraje El Pozo, (3000) Santa Fe, Argentina

## ARTICLE INFO

### Article history:

Received 5 May 2015

Received in revised form 2 June 2015

Accepted 16 June 2015

Available online 22 June 2015

### Keywords:

Cross-metathesis

Methyl oleate

1-Hexene

Hoveyda–Grubbs catalysts,

Oleochemistry

FAME

## ABSTRACT

The activity and selectivity of silica-supported Hoveyda–Grubbs (HG) complex for the cross-metathesis of methyl oleate with 1-hexene to obtain 1-decene, methyl 9-tetradecenoate, 5-tetradecene and methyl 9-decenoate were studied in a batch reactor. The HG complex loading was varied between 0.87 and 11.6 wt%. Competitive secondary reactions were the self-metathesis of methyl oleate and the self-metathesis of 1-hexene. The yield to cross-metathesis products ( $\eta_{C-M}$ ) was 47% when a 1-hexene/methyl oleate reactant ratio ( $R_{C6/MO}$ ) of one was employed. The  $\eta_{C-M}$  value increased with increasing 1-hexene initial concentration, reaching 87% for  $R_{C6/MO} = 7$ . The selectivity to terminal olefins also increased at the expense of internal olefins among the cross-metathesis products when the concentration of 1-hexene was increased.

© 2015 Elsevier B.V. All rights reserved.

## 1. Introduction

Metathesis reactions are becoming increasingly attractive in the oleochemistry industry because they offer novel routes for the valorisation of unsaturated fatty acid methyl esters (FAME) that are cheap feedstocks obtained by transesterification of natural oils and fats [1]. Homogeneous catalysis has been successfully employed for what is FAME metathesis, especially using Grubbs' Ru complexes [2] and second generation ruthenium Hoveyda–Grubbs (HG) catalysts (Fig. 1) that are remarkably tolerant to the presence of moisture and oxygen [3,4]. However, the industrial application of homogeneous olefin metathesis catalysts is hampered by the expensive catalyst separation processes needed to obtain high-purity chemicals and the contamination of products by Ru catalyst residues that are difficult to eliminate. Therefore, increasing research efforts have been made lately for developing active and stable immobilized supported complexes that allow straightforward catalyst separation and recovery. For example, commercial available Ru-alkylidene complexes immobilized on different supports have been employed without leaching or significant activity loss for olefin metathesis reactions [5,6,7]. Recently, we reported

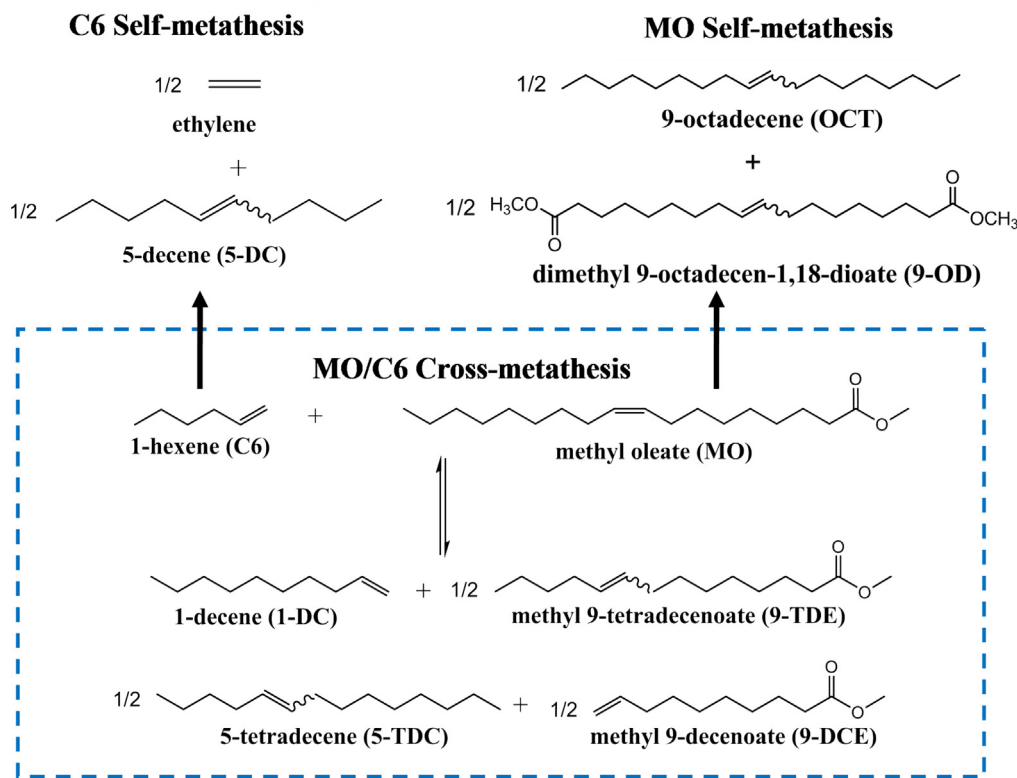
that silica-supported HG complexes are stable, highly active and selective catalysts for the self-metathesis of methyl oleate [8].

Cross-metathesis of FAME with lower olefins allows shortening of the long-chain FAME molecules to form less abundant medium-chain fatty acid esters that are valuable intermediates in fine chemistry [9]. Most of the work on cross-metathesis of oil-derived unsaturated esters with simple alkenes has been carried out using homogeneous ruthenium-based catalysts. In particular, the metathesis of methyl oleate (MO) with ethylene (ethenolysis) and with 2-butene were investigated on Ru complexes [10,11,12] while the cross-metathesis of MO with 1-hexene was studied on homogeneous  $WCl_6/(CH_3)_4Sn$  catalysts [13]. In heterogeneous catalysis, the ethenolysis of MO was performed on  $Re_2O_7/Al_2O_3$  and on  $CH_3ReO_3$  supported on  $SiO_2-Al_2O_3$  [14,15], but there are no reports on the use of immobilized Ru complexes for promoting the cross-metathesis of MO with olefins. Precisely, in this work we study the cross-metathesis of MO with 1-hexene (C6) on second generation Ru Hoveyda–Grubbs complexes supported on silica. This metathesis reaction produces 1-decene (1-DC), methyl 9-tetradecenoate (9-TDE), 5-tetradecene (5-TDC) and methyl 9-decenoate (9-DCE), as depicted in Scheme 1. 9-TDE is used for the synthesis of pheromones such as cis/trans-9-tetradecenal and cis-9-tetradecenol, which are non-toxic and biodegradable chemicals increasingly employed for the control of insect pests [16]. The synthesis route to pheromones via metathesis reactions is a one- to three-steps alternative to the current conventional technologies that employ multistep sequences [17]. 9-DCE is a valuable

\* Corresponding author. Fax: +54 342 4531068.

E-mail address: [capesteg@fiq.unl.edu.ar](mailto:capesteg@fiq.unl.edu.ar) (C.R. Apesteguía).

URL: <http://www.fiq.unl.edu.ar/gicic> (C.R. Apesteguía).



**Scheme 1.** Cross-metathesis of methyl oleate with 1-hexene and self-metathesis of methyl oleate and 1-hexene.

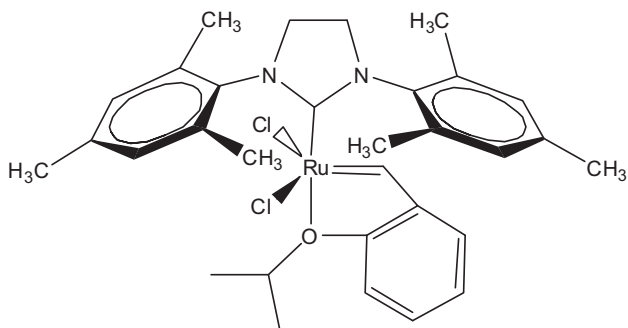


**Fig. 1.** Ru Hoveyda–Grubbs catalyst used in this work.

intermediate for the synthesis of fragrances and prostaglandins and is also employed in the polymer industry [18,19]. Secondary reactions in the MO/C6 cross-metathesis reaction network are the self-metathesis of MO that produces 9-octadecene (OCT) and dimethyl 9-octadecen-1,18-dioate (9-OD), and the self-metathesis of C6 yielding 5-decene (5-DC) and ethylene (Scheme 1). The results presented in this work show that high yields (87%) and selectivities (93%) to MO/C6 cross-metathesis products are obtained on HG/SiO<sub>2</sub> catalysts when using high C6 concentrations to suppress secondary self-metathesis reactions.

## 2. Experimental

### 2.1. Catalyst preparation and characterization

HG/SiO<sub>2</sub> catalysts were prepared by impregnating a commercial silica (Sigma–Aldrich G62, 230 m<sup>2</sup>/g, 200 mesh) with a solution of HG (Sigma–Aldrich, 97%) in cyclohexane. The silica impregnation was carried out at 298 K by stirring during 30 min; the solid colour rapidly changed from white to green and was then filtered

and dried in vacuum. HG/SiO<sub>2</sub> samples containing different HG amounts (between 0.87 wt.% HG and 11.6 wt.% HG) were prepared. The HG loading on HG/SiO<sub>2</sub> samples was determined by measuring by UV–vis spectroscopy (PerkinElmer Lambda 20 spectrophotometer) the colorimetric difference of the HG impregnating solution, before and after impregnation. The crystalline structure of the samples was determined by X-ray diffraction (XRD) using a Shimadzu XD-D1 diffractometer and Ni-filtered Cu K $\alpha$  radiation.

HG/SiO<sub>2</sub> samples were characterized by Fourier transform infrared spectroscopy (FTIR) using a Shimadzu Prestige 21 spectrophotometer. The spectral resolution was 4 cm<sup>-1</sup> and 140 scans were added. Powder samples were mixed with KBr and pressed to thin wafers. Spectra were taken at room temperature by subtracting the background spectrum recorded previously.

The interaction between the HG complex and the silica support was studied by diffuse reflectance infrared Fourier transform spectroscopy (DRIFTS) using a Shimadzu IRPrestige-21 spectrophotometer, equipped with an in-situ high-temperature/high pressure SpectraTech cell and a liquid nitrogen-cooled MCT detector. The sample holder was placed inside a dome with CaF<sub>2</sub> windows. The DRIFT spectra were collected in Ar (60 ml/min). The spectrum of silica support was previously collected. The IR spectra showed in this paper for HG/SiO<sub>2</sub> samples are the difference spectra where the SiO<sub>2</sub> spectrum served as the reference.

### 2.2. Catalytic reactions

The cross-metathesis of methyl oleate (Sigma–Aldrich, 99%) with 1-hexene (Sigma–Aldrich, 99%) was carried out at 303 K and 101.3 kPa in a glass batch reactor under Ar atmosphere. Cyclohexane (Sigma–Aldrich, anhydrous 99.5%) previously dehydrated with metallic Na and benzophenone under reflux was used as solvent. The reactor was loaded at room temperature with variable amounts of MO, C6 and catalyst together with cyclohexane (10 ml) and *n*-dodecane (internal standard). Then the reaction mixture

was stirred and heated to the reaction temperature in a thermostatic bath. Reaction products were analyzed by ex-situ gas chromatography in an Agilent 6850 GC chromatograph equipped with a flame ionization detector and a 50 m HP-1 capillary column (50 m × 0.32 mm ID, 1.05 μm film). Samples from the reaction system were collected periodically for 40–250 min. Product identification was carried out using gas chromatography coupled with mass spectrometry (Varian Saturn 2000) a VF5-HT capillary column. Besides the cross-metathesis reaction products (1-DC, 9-TDE, 5-TDC and 9-DCE) it was detected the formation of 9-OD and 9-OCT from the self-metathesis of MO, and 5-DC from the self-metathesis of C6. All the product yields were calculated in carbon basis. The yield to MO/C6 cross-metathesis products ( $\eta_{C-M}$ , C atoms of cross-metathesis products formed/C atoms of MO fed) was determined as

$\eta_{C-M} = \frac{\sum \alpha_i n_i}{\alpha_{MO} n_{MO}^0}$ , where  $n_i$  are the moles of product  $i$  formed from the cross-metathesis reaction,  $\alpha_i$  the number of C atoms of MO included in the product  $i$  molecule,  $n_{MO}^0$  the initial moles of MO, and  $\alpha_{MO}$  the number of C atoms in the MO molecule. The yield to MO self-metathesis products was obtained as  $\eta_{S-MO} = \frac{\sum \alpha_j n_j}{\alpha_{MO} n_{MO}^0}$ , where  $n_j$  are the moles of product  $j$  formed from the MO self-metathesis reaction and  $\alpha_j$  number of C atoms in the product  $j$  molecule. The yield to C6 self-metathesis products was calculated as  $\eta_{S-C6} = \frac{\sum \alpha_k n_k}{\alpha_{C6} n_{C6}^0}$ ,

where  $n_k$  are moles of product  $k$  formed from the C6 self-metathesis reaction,  $\alpha_k$  the number of C atoms in the product  $k$  molecule,  $n_{C6}^0$  the initial moles of C6, and  $\alpha_{C6}$  the number of C atoms in the C6 molecule. The selectivity to MO/C6 cross-metathesis products was obtained as  $S_{C-MO} = \frac{\eta_{C-MO}}{X_{MO}}$ , where  $X_{MO}$  is the conversion of MO; similarly the selectivities to the self-metathesis products of MO and C6 were calculated as  $S_{S-MO} = \frac{\eta_{S-MO}}{X_{MO}}$  and  $S_{S-C6} = \frac{\eta_{S-C6}}{X_{C6}}$ , respectively.

The self-metathesis of methyl oleate and 1-hexene were carried out using the same reaction unit, analysis system and operation conditions than those described above for the MO/C6 cross-metathesis reaction.

### 3. Results and discussion

#### 3.1. Catalyst characterization

The HG loading of HG/SiO<sub>2</sub> samples used in this work was between 0.87 and 11.6% wt. We determined experimentally the HG monolayer value by successively adding at 298 K small amounts of a  $0.68 \times 10^{-3}$  M HG/cyclohexane solution to 100 mg of SiO<sub>2</sub> placed in 3 ml of cyclohexane into a stirred beaker. We analyzed the supernatant solution after every HG addition by UV-vis spectroscopy following the 570 nm absorbance signal (maximum absorbance of HG complex) until detecting the presence of the HG complex. The value of the HG monolayer obtained from this experiment was about 11.6% (Fig. 2).

In Fig. 3 we present the XRD diffractograms corresponding to SiO<sub>2</sub>, HG complex [20], and HG/SiO<sub>2</sub> samples containing 0.87, 2.24, 6.0 and 11.6% HG. All the HG/SiO<sub>2</sub> samples exhibited only the amorphous halo of SiO<sub>2</sub> support. The absence of XRD peaks due to HG crystalline structure suggests that the HG complex is highly dispersed on the silica support, as it was reported previously [5].

Fig. 4 shows the FTIR spectra of HG complex, SiO<sub>2</sub>, HG(6.0%)/SiO<sub>2</sub> and HG(11.6%)/SiO<sub>2</sub> obtained in the 500–800 cm<sup>-1</sup> region. In this region, the HG complex exhibits the 748 cm<sup>-1</sup> band characteristics of the Ru=C bond stretch, and the absorption band at 580 cm<sup>-1</sup> resulting from the Ru–C vibration [21]. Both IR bands at 748 and 580 cm<sup>-1</sup> were also detected on HG/SiO<sub>2</sub> samples thereby suggesting that the HG structure was preserved after its deposition on silica.

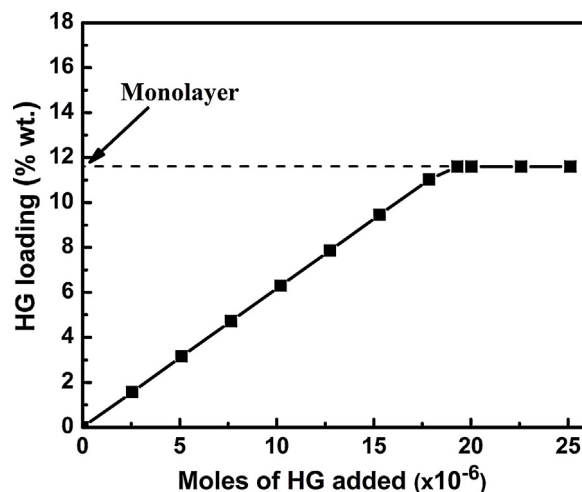


Fig. 2. Determination of the HG monolayer on SiO<sub>2</sub> support.

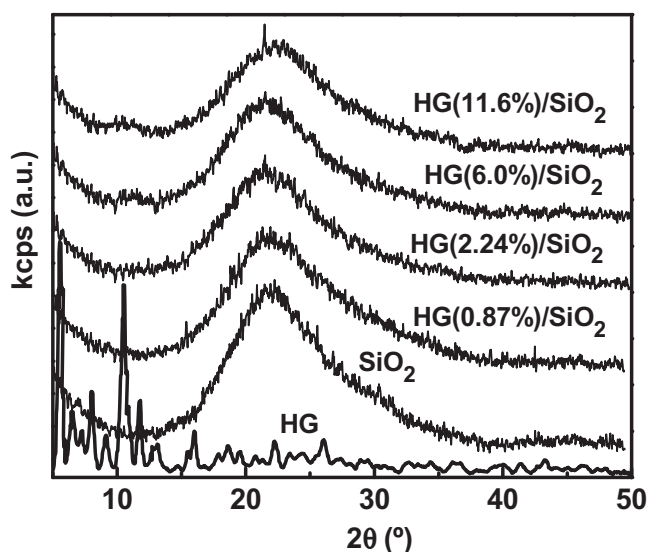


Fig. 3. XRD diffractograms of the HG complex, SiO<sub>2</sub> and HG/SiO<sub>2</sub> samples.

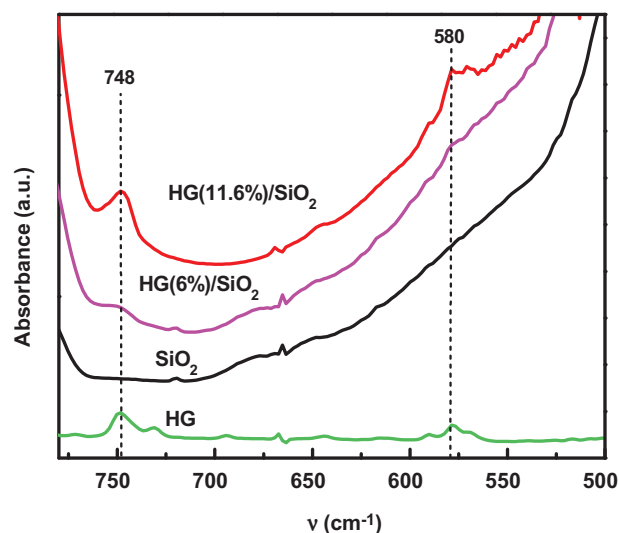


Fig. 4. FTIR spectra of the samples in the 500–800 cm<sup>-1</sup> region.

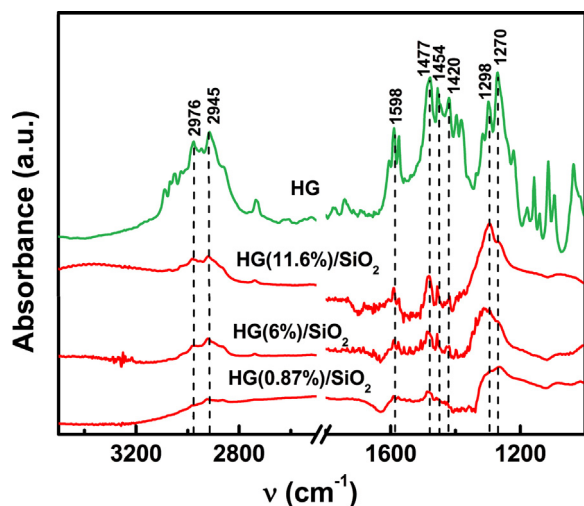


Fig. 5. DRIFT spectra of HG complex and HG/SiO<sub>2</sub> samples (0.87, 6.0 and 11.6% HG).

More knowledge on the interaction between the HG complex and the support was obtained using DRIFT spectroscopy. Spectra of the HG complex and HG/SiO<sub>2</sub> samples (0.87, 6.0 and 11.6% HG) obtained at 303 K in the 1000–3500 cm<sup>-1</sup> region, are shown in Fig. 5. In agreement with literature [22], the main absorption bands of the HG complex appeared in the 1200–1700 cm<sup>-1</sup> and 2800–3200 cm<sup>-1</sup> regions. In the 1200–1700 cm<sup>-1</sup> region, the bands at 1454 cm<sup>-1</sup>, 1392 cm<sup>-1</sup> and 1298 cm<sup>-1</sup> are attributable to  $\nu(\text{C}=\text{C})$  aromatic,  $\delta(\text{CH}_3)$  and  $\delta(\text{CH}_2)$ , respectively. In the 2800–3200 cm<sup>-1</sup> zone, the IR bands at 2945 cm<sup>-1</sup> and 2976 cm<sup>-1</sup> correspond to  $\nu(\text{CH}_3, \text{CH}_2)$  asymmetric and  $\nu(\text{CH}_3, \text{CH}_2)$  symmetric stretches. Fig. 5 shows that the main absorption bands of the HG complex appeared in the spectra of HG(6.0%)/SiO<sub>2</sub> and HG(11.6%)/SiO<sub>2</sub> samples, thereby confirming that the HG ligands and structure were conserved after the HG impregnation on the support. In contrast, the IR bands characteristics of the HG complex were not detected on HG(0.87%)/SiO<sub>2</sub>, probably because of the low HG loading.

## 3.2. Catalytic results

### 3.2.1. Self-metathesis of methyl oleate and 1-hexene

The reaction network in Scheme 1 shows that the self-metathesis of MO and C6 are detrimental secondary reactions when the research goal is to selectively produce MO/C6 cross-metathesis products. Therefore, we initially investigated the activity of HG/SiO<sub>2</sub> catalysts for both self-metathesis reactions. It is significant to note here that in a previous study of the self-metathesis of MO on HG/SiO<sub>2</sub> catalysts [8] we verified that there is not lixiviation of the HG complex when cyclohexane is used as the solvent, in agreement with results reported by other authors [5]. Details of the experiments carried out for verifying that the results obtained for metathesis reactions in cyclohexane on HG/SiO<sub>2</sub> catalysts effectively reflect the activity of immobilized HG complex are reported in [8]. Fig. 6 presents the conversion vs time curves obtained on HG(0.87%)/SiO<sub>2</sub> at 303 K. The MO conversion rapidly reached the equilibrium value of 50% [8] indicating that HG(0.87%)/SiO<sub>2</sub> is very active for the self-metathesis of MO. The self-metathesis of C6 is not limited by equilibrium because one of the reaction products, ethylene, is continuously removed from the gas phase. However, the C6 conversion on HG(0.87%)/SiO<sub>2</sub> remained almost constant ( $X_{\text{C6}} \cong 3\%$ ) after 90 min on stream, thereby suggesting a rapid in situ catalyst deactivation. The deactivation of HG-based catalysts in presence of terminal olefins has also been observed by other authors and was attributed to the low stability of methylidene intermediates leading to hydride species that suppress the metathesis cycle [23,24].

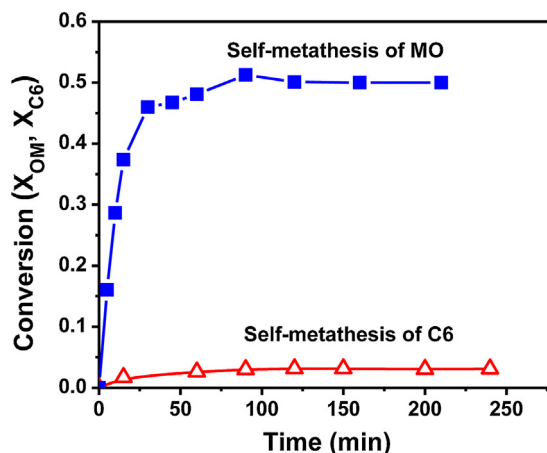


Fig. 6. Self-metathesis of methyl oleate and 1-hexene on HG(0.87%)/SiO<sub>2</sub> [ $T = 303 \text{ K}$ ,  $C_{\text{MO}}^0 = 0.029 \text{ M}$ ,  $C_{\text{C6}}^0 = 0.029 \text{ M}$ ,  $W_{\text{cat}} = 30 \text{ mg}$ , solvent: cyclohexane].

### 3.2.2. Reaction equilibrium

Cross-metathesis reactions are often limited by equilibrium. Here, we determined experimentally the equilibrium of the reaction depicted in Scheme 1 because there are no data in this regard to our knowledge. The MO/C6 cross-metathesis reaction was carried out at 303 K using dissolved HG and HG(1.12%)/SiO<sub>2</sub> catalysts. Similar HG amounts were employed in both catalytic tests; results are shown in Fig. 7. When the reaction was performed in homogeneous phase,  $X_{\text{MO}}$  remained constant after rapidly reaching a value of 0.67 (Fig. 7a); to verify that the reaction had reached the equilibrium, we added to the reactor  $5.4 \times 10^{-7} \text{ mol}$  of the HG complex after 120 min of reaction and we observed that  $X_{\text{MO}}$  was not modified by the addition of catalyst. The MO conversion on HG(1.12%)/SiO<sub>2</sub> reached initially only 51%, but following the addition of 30 mg of catalyst after 175 min of reaction  $X_{\text{MO}}$  increased to 67% and remained constant after a second addition of catalyst (Fig. 7b). From the results of Fig. 7 it is inferred that the MO equilibrium conversion for the reaction of Scheme 1, at 303 K and a reactant ratio  $R_{\text{C6}/\text{MO}} = 1$ , is 67%. By employing  $X_{\text{MO}}^{\text{Eq}} = 0.67$ , we calculated the equilibrium constant corresponding to the reaction of Scheme 1 that involves three competitive reactions: the MO/C6 cross-metathesis, the self-metathesis of MO and the self-metathesis of C6; we obtained a value of  $K_{\text{Eq}} = 0.69$ . Finally, using the  $K_{\text{Eq}}$  value of 0.69 we calculated the  $X_{\text{MO}}$  equilibrium conversions for other  $R_{\text{C6}/\text{MO}}$  ratios used in this work; the obtained  $X_{\text{MO}}^{\text{Eq}}$  values are included in Table 1.

It is worth noting here that the rapid catalyst deactivation noticed in Fig. 6 for the self-metathesis of C6 was not observed in Fig. 7b for the MO/C6 reaction on HG(1.12%)/SiO<sub>2</sub>. This result strongly suggests that the competitive interaction between MO and C6 for the HG(1.12%)/SiO<sub>2</sub> active sites decreases the rate of deactivation reaction that takes place when 1-hexene is the only reaction reactant.

### 3.2.3. Cross-metathesis of methyl oleate with 1-hexene

We initially studied the effect of the HG loading on the MO conversion rate for the cross-metathesis of MO with C6 using HG/SiO<sub>2</sub> catalysts containing between 2.24 and 3.36% HG. Fig. 8 shows the evolution of  $X_{\text{MO}}$  as a function of parameter  $tW_{\text{HG}}/n_{\text{MO}}^0$  (hg<sub>HG</sub>/mol) where  $t$  is the reaction time,  $W_{\text{HG}}$  is the HG loading, and  $n_{\text{MO}}^0$  are the initial moles of MO. The local slope of each curve in Fig. 8 gives the MO conversion rate at a specific value of MO conversion and reaction time. The curves of Fig. 8 exhibited the same initial slopes, i.e. the same initial MO conversion rates ( $r_{\text{MO}}^0$ , mol/hg<sub>HG</sub>). This result reveals that the HG complex deposited on silica was completely accessible and active for promoting the MO/C6 cross-metathesis

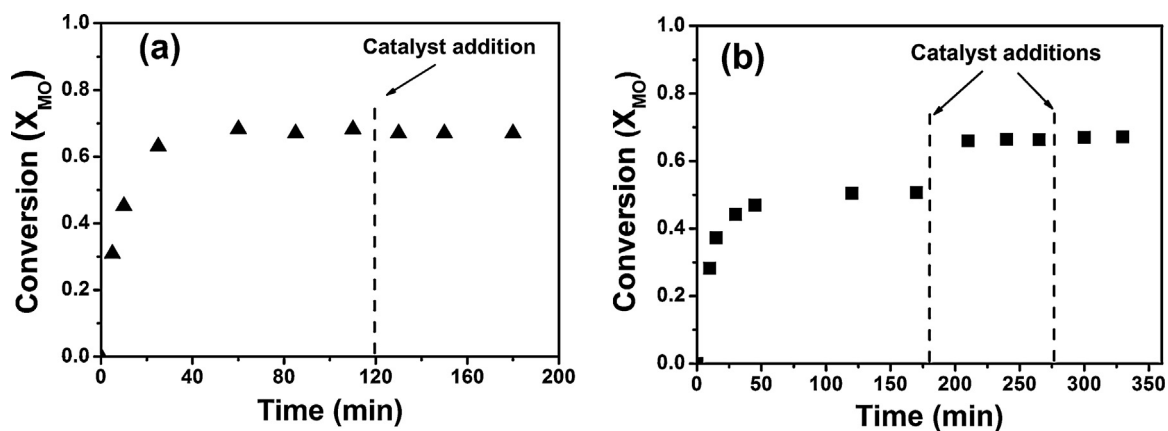


Fig. 7. Cross-metathesis of methyl oleate with 1-hexene. (a) Catalyst: HG (dissolved), 0.336 mg; (b) Catalyst: HG(1.12%)/SiO<sub>2</sub>, 30 mg [ $T=303$  K,  $C_{MO}^0 = 0.029$  M,  $R_{C6/MO} = 1$ ,  $R_{C6/HG} = 540$ , solvent: cyclohexane].

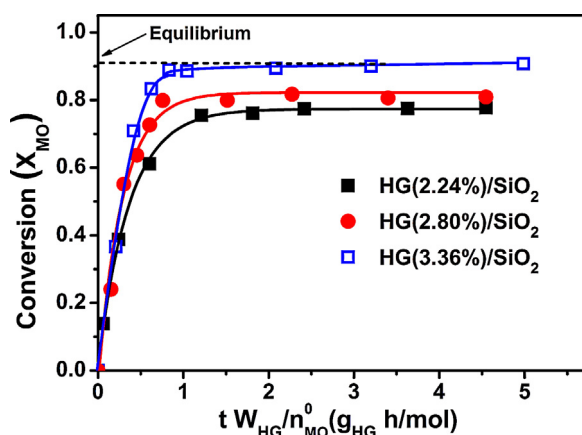


Fig. 8. Cross-metathesis of methyl oleate with 1-hexene: Effect of %HG [ $T=303$  K,  $W_{cat} = 100$  mg,  $C_{MO}^0 = 0.029$  M,  $R_{C6/MO} = 5$ , solvent: cyclohexane].

reaction. The  $r_{MO}^0$  value determined from the curves of Fig. 8 was 2.4 mol/h  $g_{HG}$ . On HG(3.36%)/SiO<sub>2</sub>,  $X_{MO}$  rapidly reached the equilibrium value for  $R_{C6/MO} = 5$  (91%). In contrast,  $X_{MO}$  attained only 81% and 77% on HG(2.80%)/SiO<sub>2</sub> and HG(2.24%)/SiO<sub>2</sub>, respectively, thereby indicating that both samples were deactivated during the progress of the reaction, probably because of the presence of 1-hexene as it was observed for the C6 self-metathesis reaction in Fig. 6.

Additional MO/C6 cross-metathesis catalytic runs were performed on HG(3.36%)/SiO<sub>2</sub> at 303 K to determine the reaction order

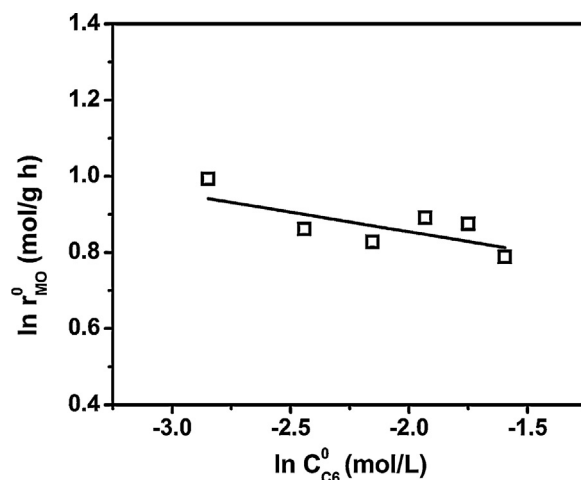


Fig. 9. Dependence of MO conversion rate upon C6 concentration [ $T=303$  K,  $W_{cat} = 100$  mg,  $C_{MO}^0 = 0.029$  M, solvent: cyclohexane].

with respect to 1-hexene. The reaction order was obtained from Eq. 1 that represents the initial MO conversion rate:

$$r_{MO}^0 = k(C_{C6}^0)^\alpha (C_{MO}^0)^\beta \quad (1)$$

The dependence of  $r_{MO}^0$  upon C6 was studied by varying C6 between 0.058 and 0.203 mol/L at  $C_{MO}^0 = 0.029$  mol/L. The plot representing  $\ln r_{MO}^0$  as a function of  $\ln C_{C6}^0$  is shown in Fig. 9. Reaction order  $\alpha$  determined from the logarithmic plot of Fig. 9 was slightly negative, about  $-0.1$ .

Table 1  
Cross-metathesis of methyl oleate with 1-hexene. Catalytic results on HG(3.36%)/SiO<sub>2</sub>.

Reactant ratio	Initial C6 concentration	Equilibrium conversion	Conversion <sup>a</sup>		Yield <sup>a</sup>			Selectivity <sup>a</sup>			Carbon balance
$R_{C6/MO}^b$	$C_{C6}^0$ (mol/L)	$X_{MO}^{eq}$ (%)	$X_{MO}$ (%)	$X_{C6}$ (%)	$\eta_{C-M}$ (%)	$\eta_{S-MO}$ (%)	$\eta_{S-C6}$ (%)	$S_{C-M}$ (%)	$S_{S-MO}$ (%)	$S_{S-C6}$ (%)	CB (% C)
1	0.029	67	67	66	46	21	23	59	41	34	94
2	0.058	75	75	61	55	20	22	73	27	37	96
3	0.087	84	84	56	69	15	20	82	18	39	95
4	0.016	88	88	50	78	10	22	89	11	44	97
5	0.145	91	91	40	83	8	19	91	9	48	95
6	0.174	96	92	34	86	6	17	93	7	50	95
7	0.203	97	93	28	87	6	15	93	7	54	99

$T=303$  K;  $C_{MO}^0 = 0.029$  M,  $W_{cat} = 100$  mg, cyclohexane (10 ml).

<sup>a</sup> At the end of catalytic runs.

<sup>b</sup> Molar ratio.

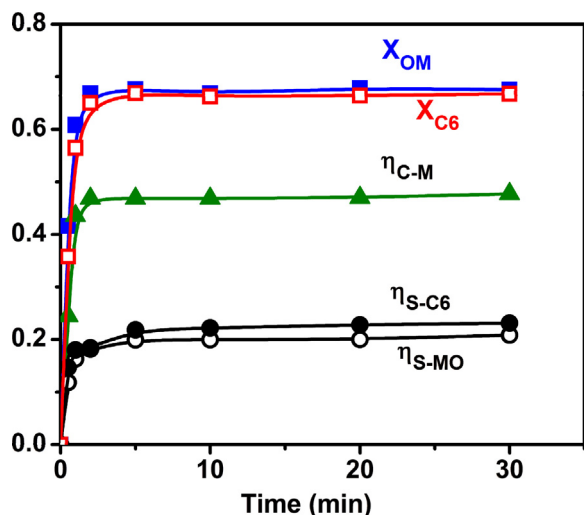


**Fig. 10.** Evolution as a function of time of MO and C6 conversions ( $X_{MO}$ ,  $X_{C6}$ ) and yields to cross-metathesis ( $\eta_{C-M}$ ), MO self-metathesis ( $\eta_{S-MO}$ ) and C6 self-metathesis ( $\eta_{S-C6}$ ) products [catalyst: HG(3.36%)/SiO<sub>2</sub>,  $T = 303$  K,  $W_{cat} = 100$  mg,  $C_{MO}^0 = 0.029$  M,  $R_{C6/MO} = 1$ , solvent: cyclohexane].

The effect of the  $R_{C6/MO}$  reactant ratio on the MO/C6 cross-metathesis reaction was studied on HG(3.36%)/SiO<sub>2</sub> at 303 K, using the same initial MO concentration,  $C_{MO}^0 = 0.029$  M;  $R_{C6/MO}$  was varied between 1 and 7. In Fig. 10 we show the evolution as a function of time of MO and C6 conversions ( $X_{MO}$ ,  $X_{C6}$ ) and yields to cross-metathesis ( $\eta_{C-M}$ ), MO self-metathesis ( $\eta_{S-MO}$ ) and C6 self-metathesis ( $\eta_{S-C6}$ ) products obtained for  $R_{C6/MO} = 1$ . When

$X_{MO}$  reached the equilibrium (67%), the  $\eta_{C-M}$  and  $\eta_{S-MO}$  values were 46 and 21%, respectively. With the aim of improving the yield to cross-metathesis products, we decided to perform additional runs at increasing  $R_{C6/MO}$  reactant ratios. We speculated that  $\eta_{C-M}$  may increase by increasing the C6 concentration because of the following reasons: i) the equilibrium of the MO/C6 cross-metathesis reaction is shifted to higher MO conversions when  $R_{C6/MO}$  is increased; ii) the rate of MO self-metathesis probably will diminish with C6 concentration because the competitive C6 interaction with the catalyst would reduce the pairs of adjacent surface active sites required for promoting this reaction. The values of MO and C6 conversions, yields, selectivities and carbon balances obtained at the end of the runs for  $R_{C6/MO}$  reactant ratios between 1 and 7 are presented in Table 1. As shown in Table 1, the MO equilibrium conversion increases from 67% ( $R_{C6/MO} = 1$ ) to 97% ( $R_{C6/MO} = 7$ ); the MO conversions obtained in the catalytic runs reached the  $X_{MO}^{eq}$  values for  $R_{C6/MO}$  between 1 and 5 and close to  $X_{MO}^{eq}$  for  $R_{C6/MO}$  6 and 7.  $\eta_{C-M}$  increased from 46% ( $R_{C6/MO} = 1$ ) to 87% ( $R_{C6/MO} = 7$ ) at the expense of  $\eta_{S-MO}$ , thereby confirming that the self-metathesis of MO is inhibited when the C6 concentration is increased. Consistently, the selectivity to cross-metathesis products,  $S_{C-M}$ , increased from 59 to 93% when  $R_{C6/MO}$  was varied from 1 to 7. As expected, the yield and selectivity to C6 self-metathesis products increased with increasing C6 concentration. In all the cases, the carbon balance was  $\geq 94\%$ .

In Fig. 11 we present the  $\eta_i$  vs time curves obtained for four different  $R_{C6/MO}$  ratios (2, 4, 5 and 7), where  $\eta_i$  is the yield of product  $i$  formed from the conversion of MO via either the MO/C6 cross-metathesis or the MO self-metathesis. The yields to 9-OCT and 9-OD, the products of self-metathesis of MO, clearly decreased

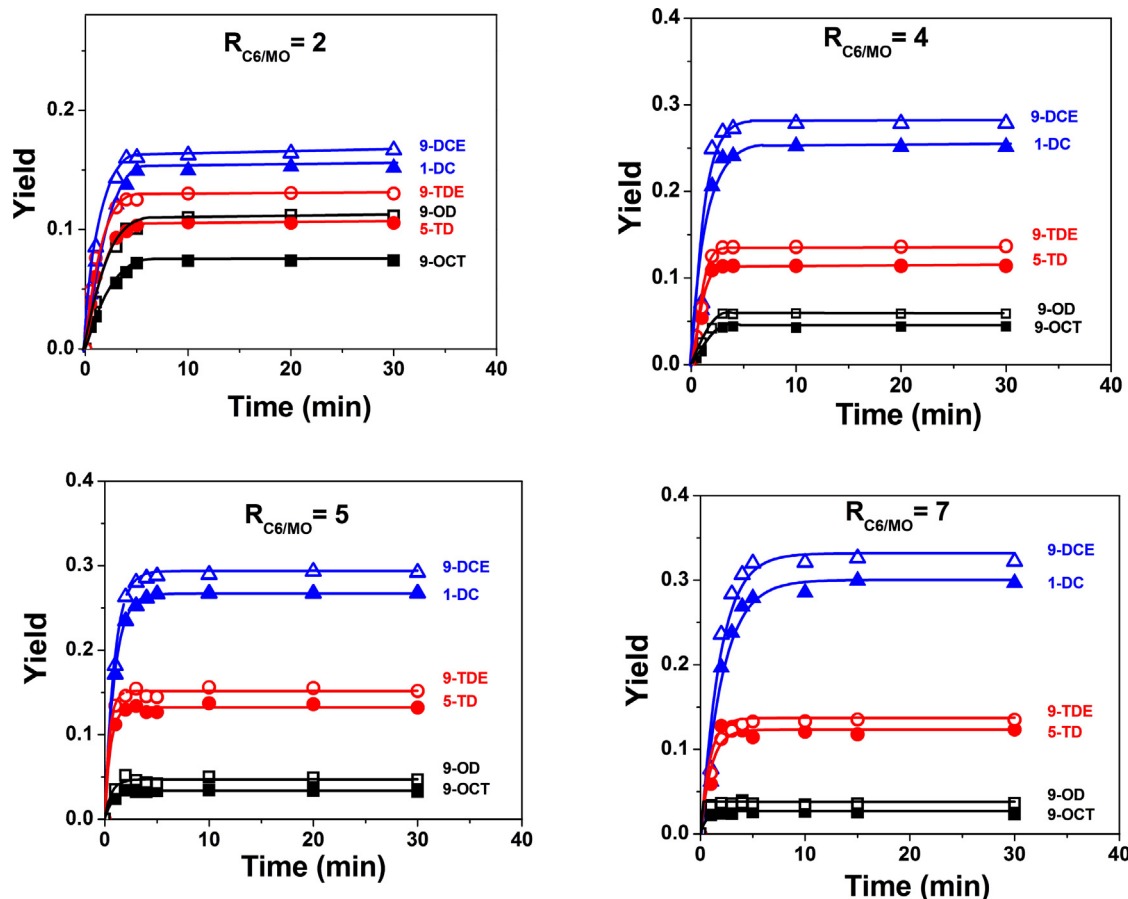


**Fig. 11.** Effect of  $R_{C6/MO}$  ratio on product distribution [catalyst: HG(3.36%)/SiO<sub>2</sub>,  $T = 303$  K,  $C_{MO}^0 = 0.029$  molar,  $W_{cat} = 100$  mg, solvent: cyclohexane].

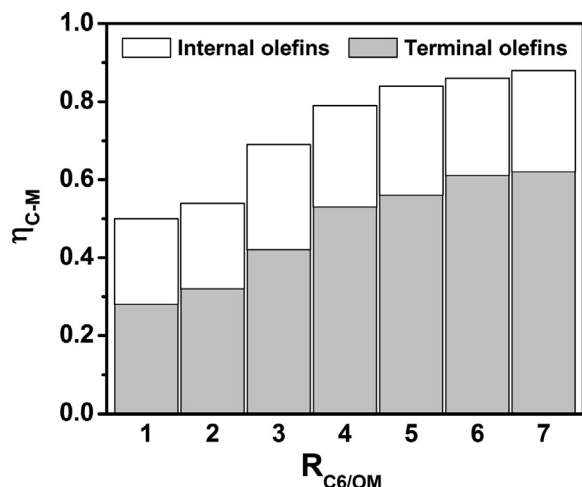


**Fig. 12.** Yields of terminal (9-DCE, 1-DC) and internal (5-TDC, 9-TDE) olefins as a function of  $R_{C6/MO}$  [Catalyst: HG(3.36%)/SiO<sub>2</sub>  $T=303$  K;  $C_{MO}^0 = 0.029$  molar,  $W_{cat} = 100$  mg, solvent: cyclohexane].

when  $R_{C6/MO}$  was increased. Regarding the MO/C6 cross-metathesis products, Fig. 11 reveals that the yield to terminal olefins 1-DC and 9-DCE increases while that to internal olefins 9-TDE and 5-TDC remains almost constant when  $R_{C6/MO}$  is increased. In Fig. 12 we have represented the yield to MO/C6 cross-metathesis products as a function of  $R_{C6/MO}$ , discriminating between terminal and internal olefins. The yield to terminal olefins increased from 28% ( $R_{C6/MO}=1$ ) to 62% ( $R_{C6/MO}=7$ ); in contrast, the yield to internal olefins oscillated between 23 and 27% in this  $R_{C6/MO}$  range. The preferential formation of terminal olefins among the MO/C6 cross-metathesis products with  $R_{C6/MO}$  is probably related to the concomitant increase of the concentration of C6 self-metathesis products, in particular ethylene (Table 1). In fact, the concentration of 5-DC increased from  $3.7 \times 10^{-3}$  mol/L ( $R_{C6/MO}=1$ ) to  $13.5 \times 10^{-3}$  mol/L ( $R_{C6/MO}=7$ ) and similar ethylene amounts are formed from C6 self-metathesis reaction (Scheme 1). The consecutive metathesis of ethylene with internal olefins 9-TDE and 5-TDC would produce then C6 and terminal olefins 1-DC and 9-DCE. In summary, increasing the C6 concentration improves the yield and selectivity to MO/C6 cross-metathesis products, in particular to terminal olefins.

However, results in Fig. 8 and Table 1 (columns 3 and 4) indicate that the deactivation of HG/SiO<sub>2</sub> catalysts becomes significant

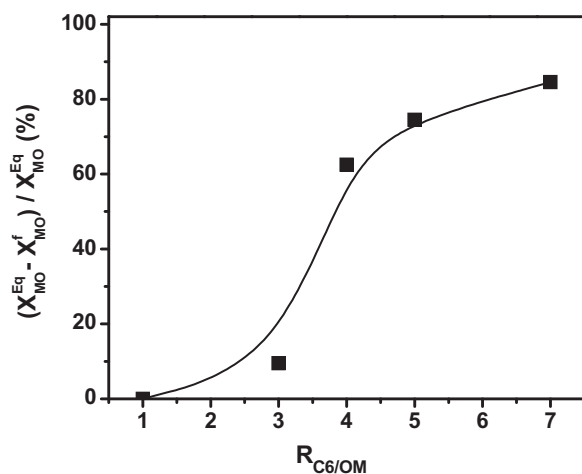


**Fig. 13.** MO/C6 cross-metathesis: deactivation of HG(1.12%)/SiO<sub>2</sub> as a function of  $R_{C6/MO}$  [ $T=303$  K;  $W_{cat} = 100$  mg,  $C_{MO}^0 = 0.029$  molar, solvent: cyclohexane].

when high  $R_{C6/MO}$  ratios are used. In order to gain more knowledge on the effect of  $R_{C6/MO}$  on catalyst deactivation, we performed additional catalytic runs of the MO/C6 cross-metathesis reaction using HG(1.12%)/SiO<sub>2</sub> catalysts. We employed the parameter  $\frac{(X_{MO}^{Eq} - X_{MO}^f)}{X_{MO}^{Eq}}$  as a quantitative measure of catalyst deactivation, where  $X_{MO}^f$  is the OM conversion achieved at the end of the 120-min runs. Results are presented in Fig. 13 and show that the HG complex is deactivated during the progress of the reaction. The catalyst deactivation increased with  $R_{C6/MO}$  ratio, which supports the assumption that the presence of terminal olefins may suppress the metathesis cycle on HG-based catalysts, as noted above. Fig. 13 also suggests that deactivation of HG/SiO<sub>2</sub> catalysts may be critical when  $R_{C6/MO}$  ratios higher than three are employed.

#### 4. Conclusions

The selective synthesis of methyl oleate/1-hexene cross-metathesis products (1-decene, methyl 9-tetradecenoate, 5-tetradecene and methyl 9-decenoate) on HG/SiO<sub>2</sub> catalysts is improved by using high 1-hexene/methyl oleate ratios. The increase of 1-hexene concentration shifts the reaction equilibrium to high MO conversion equilibrium values and concomitantly suppresses the MO self-metathesis competitive reaction. Thus, the yield and selectivity to MO/C6 cross-metathesis products reported in this work on HG(3.36%)/SiO<sub>2</sub> for a  $R_{C6/MO}$  ratio of seven are 87% and 93%, respectively. The product distribution also depends on  $R_{C6/MO}$  ratio; in fact, the yield to terminal olefins (9-decenoate, 1-decene) increases from 28% ( $R_{C6/MO}=1$ ) to 62% ( $R_{C6/MO}=7$ ) while that of internal olefins (9-tetradecenoate, 5-tetradecene) does not change significantly. Nevertheless, deactivation of HG/SiO<sub>2</sub> catalysts also increases with 1-hexene concentration and for C6/OM reactant ratios higher than three becomes more pronounced.

#### Acknowledgement

Authors thank the Universidad Nacional del Litoral (UNL), Consejo Nacional de Investigaciones Científicas y Técnicas (CONICET), and Agencia Nacional de Promoción Científica y Tecnológica (ANPCyT), Argentina, for the financial support of this work.

#### References

- [1] J.C. Mol, Top. Catal. 27 (2004) 97–104.
- [2] T.M. Trnka, R.H. Grubbs, Acc. Chem. Res. 34 (2001) 18–29.
- [3] S.B. Garber, J.S. Kingsbury, B.L. Gray, A.H. Hoveyda, J. Am. Chem. Soc. 122 (2000) 8168–8179.
- [4] S. Gessler, S. Randl, S. Blechert, Tetrahedron Lett. 41 (2000) 9973–9976.
- [5] B. Van Berlo, K. Houthoofd, B.F. Sels, P.A. Jacobs, Adv. Synth. Catal. 350 (2008) 1949–1953.
- [6] H. Balcar, T. Shinde, N. Zilkova, Z. Bastl, Beilstein J. Org. Chem. 7 (2011) 22–28.
- [7] T. Shinde, N. Zilkova, V. Hankova, H. Balcar, Catal. Today 179 (2012) 123–129.
- [8] J. Zelin, A.F. Trasarti, C.R. Apesteguía, Catal. Comm. 42 (2013) 84–88.
- [9] A. Rybank, M.A.R. Meier, Green Chem. 9 (2007) 1356–1361.
- [10] A. K. Burdett, L.D. Harris, P. Margl, B.R. Maughon, T. Mokhtar-Zadeh, P.C. Saucier, E.P. Wasserman, Organometallics 23 (2004) 2027–2047.
- [11] R.M. Thomas, B.K. Keitz, T.M. Champagne, R.H. Grubbs, J. Am. Chem. Soc. 133 (2011) 7490–7496.
- [12] J. Patel, S. Mujcinovic, W. Roy Jackson, A.J. Robinson, A.K. Serelis, C. Such, Green Chem. 8 (2006) 450–454.
- [13] B. Matyska, A. Dosedlova, L. Petrusova, H. Balcar, Collect. Czech. Chem. Commun. 54 (1989) 455–461.
- [14] M. Sibeijn, J.C. Mol, J. Mol. Catal. 76 (1992) 345–358.
- [15] D. Mandelli, M.J.D.M. Jannini, R. Buffon, U. Schuchardt, J. Am. Oil Chem. Soc. 73 (1996) 229–232.
- [16] J. Gillespie, S. Herbig, R. Beyerinck, in: F.R. Hall, J.W. Barry (Eds.), Biorational Pest Control Agents, 595, ACS Symposium Series, 1995, pp. 208–212.
- [17] D. Banasiak, J. Mol. Catal. 28 (1985) 107–115.
- [18] C. J. Mol, J. Mol. Catal. 90 (1994) 185–199.
- [19] C. J. Mol, Green Chem. 4 (2002) 5–13.

- [20] G. Wilson, M. Caruso, N. Reimer, S. White, N. Sottos, J. Moore, *Chem. Mater.* 20 (2008) 3288–3297.
- [21] S. Garber, J. Kingsbury, B. Gray, A. Hoveyda, *J. Am. Chem. Soc.* 122 (2000) 8168–8179.
- [22] A. Keraani, C. Fischmeister, T. Renouard, M. Le Floch, A. Baudry, C. Bruneau, M. Rabiller-Baudry, *J. Mol. Catal. A Chem.* 357 (2012) 73–80.
- [23] J.W. van Rensburg, P.J. Steynberg, W.H. Meyer, M.M. Kirk, G.S. Forman, *J. Am. Chem. Soc.* 126 (14) (2004) 332–14333.
- [24] H. Hong, A. Wenzel, T. Salguero, M. Day, R. Grubbs, *J. Am. Chem. Soc.* 129 (2007) 7961–7968.